Chapter 3: Understanding the Pacific Fracture Zones

Abstract

Nine fracture zones running roughly east west on the Pacific Ocean floor generally defined as transform faults are analyzed as portions of small circle escarpments comparable to Altai scarp in the third ring of Mare Nectarous on the moon. Structurally they resemble the Altai scarp and bear no resemblance to the San Andreas Fault, the typical example of a transform fault, having no evidence of seismic activity in their structure.

Key words: Pacific Fracture Zones, Clarion Fracture Zone, Altai Escarpment, shock-release wave.

Introduction

Plate tectonics was first proposed by Antonio Snider in 1859 connecting it to crustal plates moving during the Flood (Austin et al 2010). Frank Taylor renewed the idea in 1910 (Hoffman 2014) when he saw stress trends in the Alps and Himalayas. He proposed that Europe and Asia were dragged towards the equator during the Cenozoic by increased lunar gravity. In 1912 Alfred Wegener spoke of "Carboniferous Pangea and its subsequent fragmentation and dispersal" (page 197). From these papers grew up the idea of "continental drift."

Tuzo Wilson gave Plate Tectonics (PT) much of its present shape with the 1965 paper, "A new class of faults and their bearing on Continental Drift". At that time developing knowledge of the sea floor had identified the Pacific Fracture Zones (PFZ) as multiple trench and ridge systems, 4,000-12,000 km (2,500-7,500 miles) long, crossing the Pacific Basin roughly from east to west.

Wilson proposed a new type of fault that transformed "the horizontal sheer motion along the [transforming] fault … by being changed into an expanding tensional motion across the ridge or rift with a change in seismicity" (Wilson 1965, page 343). As we have learned more about the ocean floor, does this 1965 interpretation of the PFZ in the context of PT hold up to our current knowledge of their structure?

Trough-ridge system as a transform fault

Wilson's prime example of a transform fault was the San Andreas Fault, probably the most famous plate boundary in the world, where the North American and Pacific Plates meet at the edge of California, USA. The Pacific plate appears to be moving northward, compared to the North American plate, at about 2 inches (5 cm) a year. This movement expands outwards through seismicity from the San Andreas Fault proper through smaller connected faults to form a wide trend known as California's earthquake zone, showing no orderly elevation changes.

While Wilson did not name the Pacific FZ specifically as a transform faults, he did suggest the Pacific Plate was rotating, and Morgan (1968) applied the nomenclature of transform faults to the Pacific FZ. Wilson (1965) had postulated transform faults in the South Atlantic separated portions of the plate that move at different rates, sliding against each other *without any ocean crust being modified* (conservative plate boundaries) and leaving orderly elevation changes (in sharp contrast to his prime example, the San Andreas Fault) for short distances while they connect oceanic ridges (divergent boundaries) to ocean trenches (convergent boundaries).

Morgan (1968) recognized that movement of one plate on a sphere would be rotational relative to another plate, and any rotating plate would rotate around a single point. Lines produced by that rotation would show small circle relationships. He calculated the Pacific FZ were long rotational fractures with a small circle relationship around a rotational center, Euler Pole, at 79^{o}N, 111^{o}E. But they exhibited none of the seismicity of the San Andreas and show orderly elevation changes. Wilson stated, "Transform faults cannot exist unless there is crustal displacement, and their existence would provide a powerful argument in favor of continental drift and a guide to the nature of the displacement" (page 344). That is a good theoretical statement, but the Pacific FZ's trough-ridges show elevation change without associated earthquake or volcanic activity. If PT causes elevation change through seismicity then this trough-ridge system must have another origin.

Bathymetry of the trough-ridge system

In the mid 1960's the ocean floors were largely still unexplored territory. While the general shape and location of the PFZ was known by 1968 (Morgan 1968); it was under appreciated. Another aerial pattern and profile of a smaller ridge system roughly parallel to the California coast at the edge of the Pacific and North American plates was of greater interest at that time. The small ridge system was accompanied by a magnetic anomaly pattern that Atwater (1970) associated with the San Andreas Fault and considered to be the most prominent geomorphology in that area. The Pacific FZ are roughly perpendicular to the San Andreas, so Atwater assumed they were transverse faults to the ridge's magnetic anomaly. The 1968 National Geographic "Pacific Floor" and the 1981 "World Ocean Floor" painted maps show prominent N-S ridges filling the ocean floor's surface between Pacific FZ. While this pattern reflected the expectations of PT and portrayed the Pacific's floor to resemble the Atlantic's, verifying this structure with Google Earth shows differently. The NOAA (National Oceanic and Atmospheric Administration) data that fills the ocean floor of the Central Pacific (Figure 3.1) has only a few E-W mountain linears, while the Central Atlantic Ocean has about the same numbers of linears trending N-S as trending E-W.

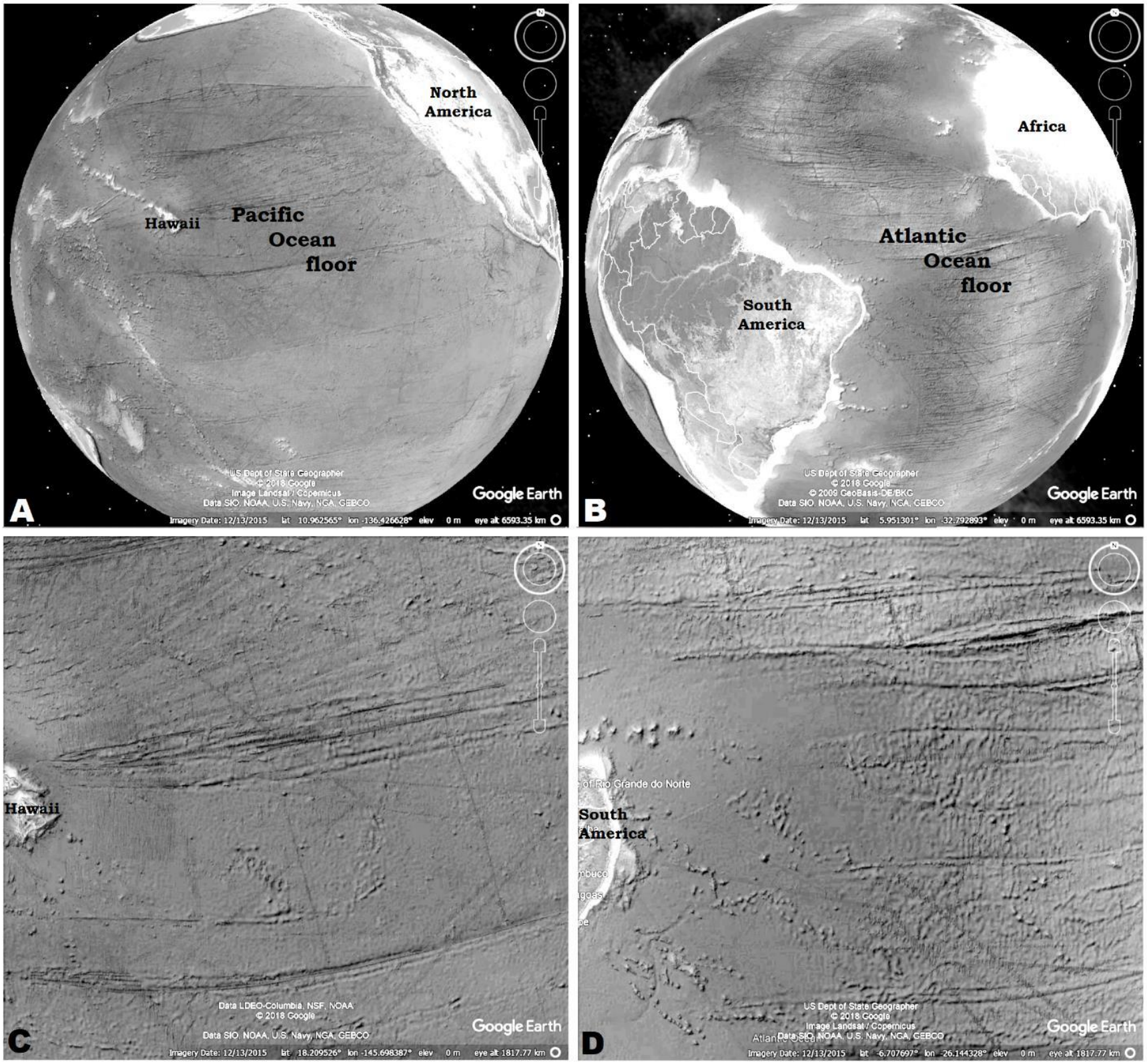

Figure 3.1: The Pacific and Atlantic Oceans, showing the bathymetry data from satellite. C and D are details of A and B respectively. Color adjusted to remove the dense blue and increase contrast. (Image credit: NOAA displayed in Google Earth.)

Between the words “Mendocino FZ” and “Murry FZ” in Figure 3.2 are small red arrows pointing to the ridges that Atwater saw in that area, and contrast them with the visibility and size of the PFZ marked with pairs of black arrows. It is clear the PFZ are the more dominant land form. Where several parallel ridges and troughs occur, such as the Molokai FZ, the plate is believed to have been moving slower, and when only one ridge is obvious, like in the Clarion or Murry FZs, the plate is believed to have been moving more rapidly (Atwater 1970, Atwater et al 1993, Austermann et al 2011). Where the Pacific FZ lines wobble, the center of rotation is believed to have shifted. But, no reason is given for how ridge-valley forms were conserved in these lines over such great distances.

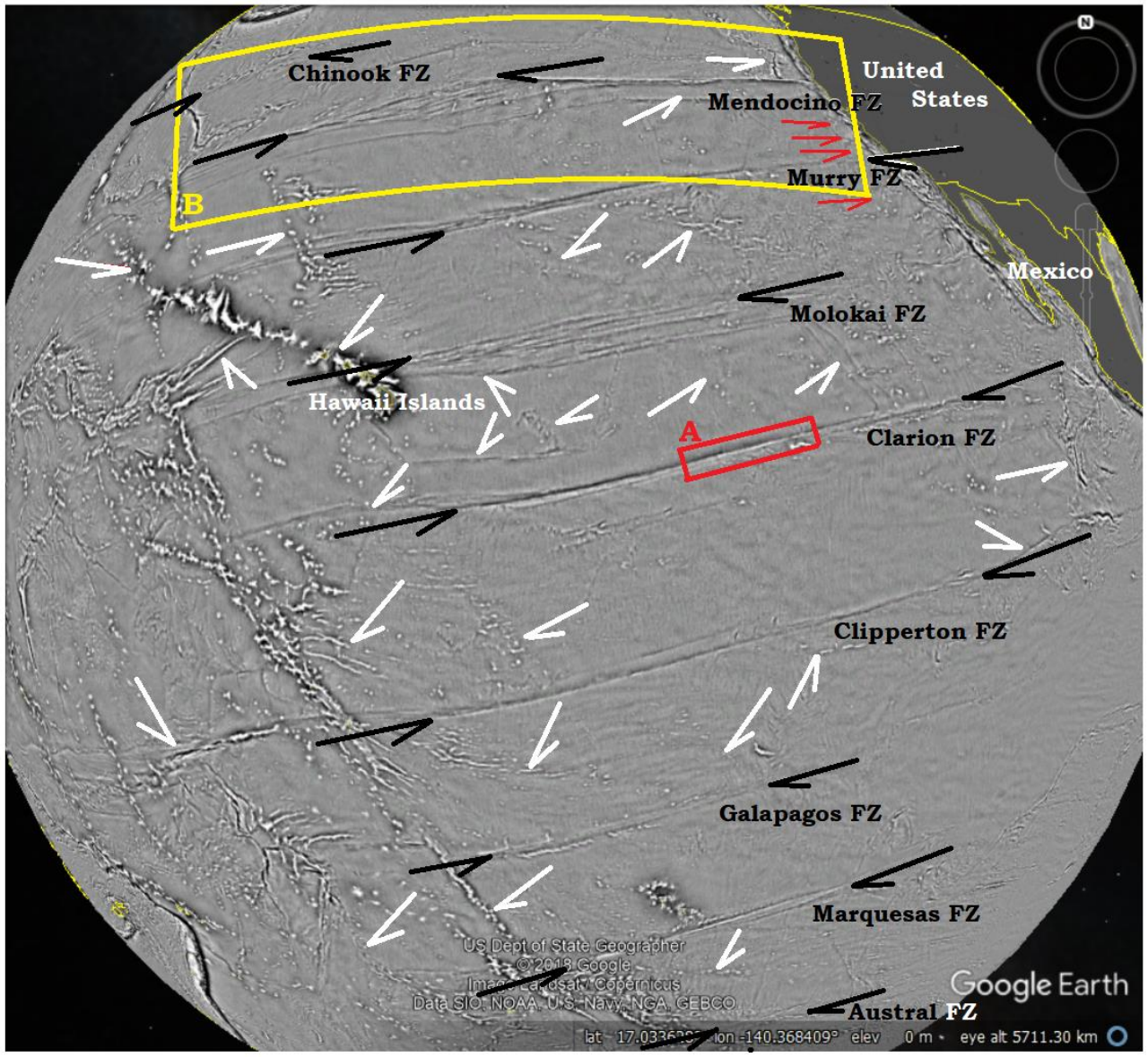

Figure 3.2: Vertical Gravity Gradient overlay for Google Earth, showing bathymetric structure derived from satellite of the Pacific Ocean with the Fracture Zones for this paper marked with black arrows at each ends of the segments considered. White arrows pointing obliquely at other linears. (2017 Google Earth.)

Structure of the PFZ

Several of the Pacific Fractures Zone have been imaged in cross section both topographic and gravity at significant resolution from shipboard. Figure 3.3B shows a close-up view of area A in Figure 3.2. Figure 3.3C shows a detail of 3B and location for the cross sections of Figure 3.4. The cross section of the Clarion FZ is typical of many of the PFZ and shows the classic form of a shock-release wave (Figure 1.3) derived from laser surgery (Teubner et al 2017) to mathematical models for large astral- impactors (Jones et al 2002).

Plate tectonics has an explanation for the high-low shape of the Pacific FZ. Morgan (1968) portrays the center of the rise, about where the transition from red to blue occurs in Figure 3.4, as the point of slip between the edge of an inner plate, low trough, that is moving/ expanding more slowly, and the outer portion of the plate, high escarpment, which is expanding more rapidly. McCarthy et al (1996, page 13,715) explains it this way, “Younger-side lithosphere flexes up at the fault, while older-side lithosphere flexes down at the fault, producing a characteristic high-low pair….”

This explanation is inadequate. What flexed? Why did its lithology flex without any accompanying seismicity? Why is there no visible joint where the slide between plate sections took place? If there is a joint where the plates are believed to slide past each other, as in the San Andreas Fault, why is there not a visible fault-joint here?

Looking at the Clarion cross section 2, Figure 3.4, within 120 km (75 mi) the fracture zone registers the extremely escarpment of the ridge, about 2000 m (1.2 mi) tall then slides rapidly into the trough depths, 1000 m (0.6 mi), for a total change of about 3 km. (1.86 mi.). That rapid energy difference from the high to the low is typical of an adiabatic energy exchange, Figure 1.1. It happens too rapidly for most of the energy to be transferred from molecule to molecule so the excess of energy is converted to work, causing separation of the molecules and vaporization of the substrate. I will refer to this energy exchange as an adiabatic envelope producing reduced pressure and disrupted substrate. As the wave’s energy is centered down in the substrate and as the shock wave continues to pass, the substrate is no longer able to contain the integrity of the greatly raising substrate under the effect of the adiabatic shift between shock and release waves, and when the adiabatic envelope burst, the release wave valley is left. One measurement of this shift in a microscopic laser generated shock wave, the supersonic speed reached Mach 6, which converts to ~30 GPa. (Pezeril et al 2011). This drastic energy change occurs within a *few millimeters* in eye surgery applications.

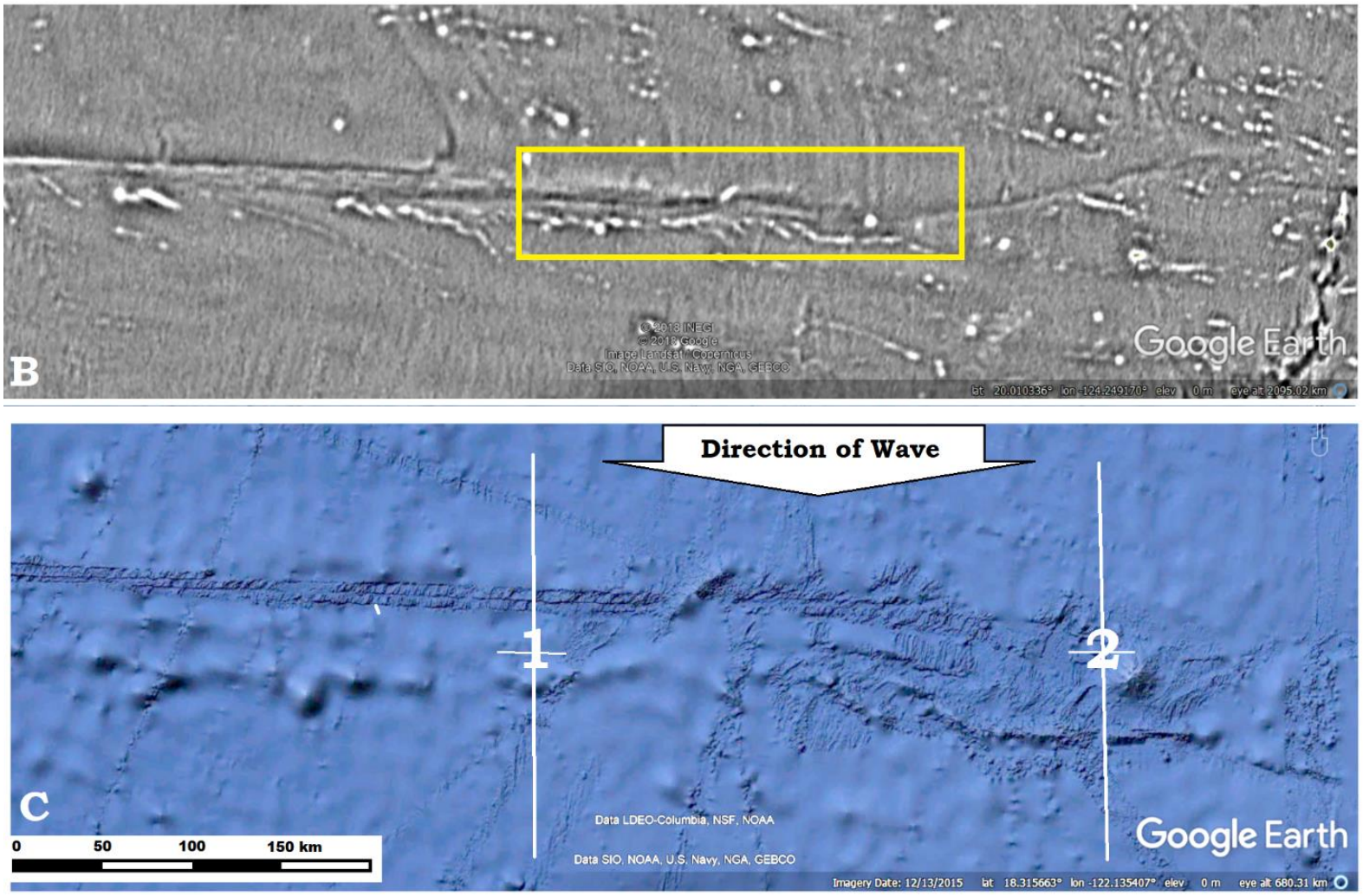

Figure 3.3: Details of the Clarion FZ at greater resolution. Starting with A in Figure 3.2, B is shown in Vertical Gravity Gradient and indicates the location of detail C in yellow. “C” is NOAA data from Google Earth color modified to remove some of the dark blue Google Earth adds to the ocean basins. The approximate locations of cross sections 1 and 2 are shown C. (“Tank tracks” are paths of greater know detail from shipping lanes not additional structure.)

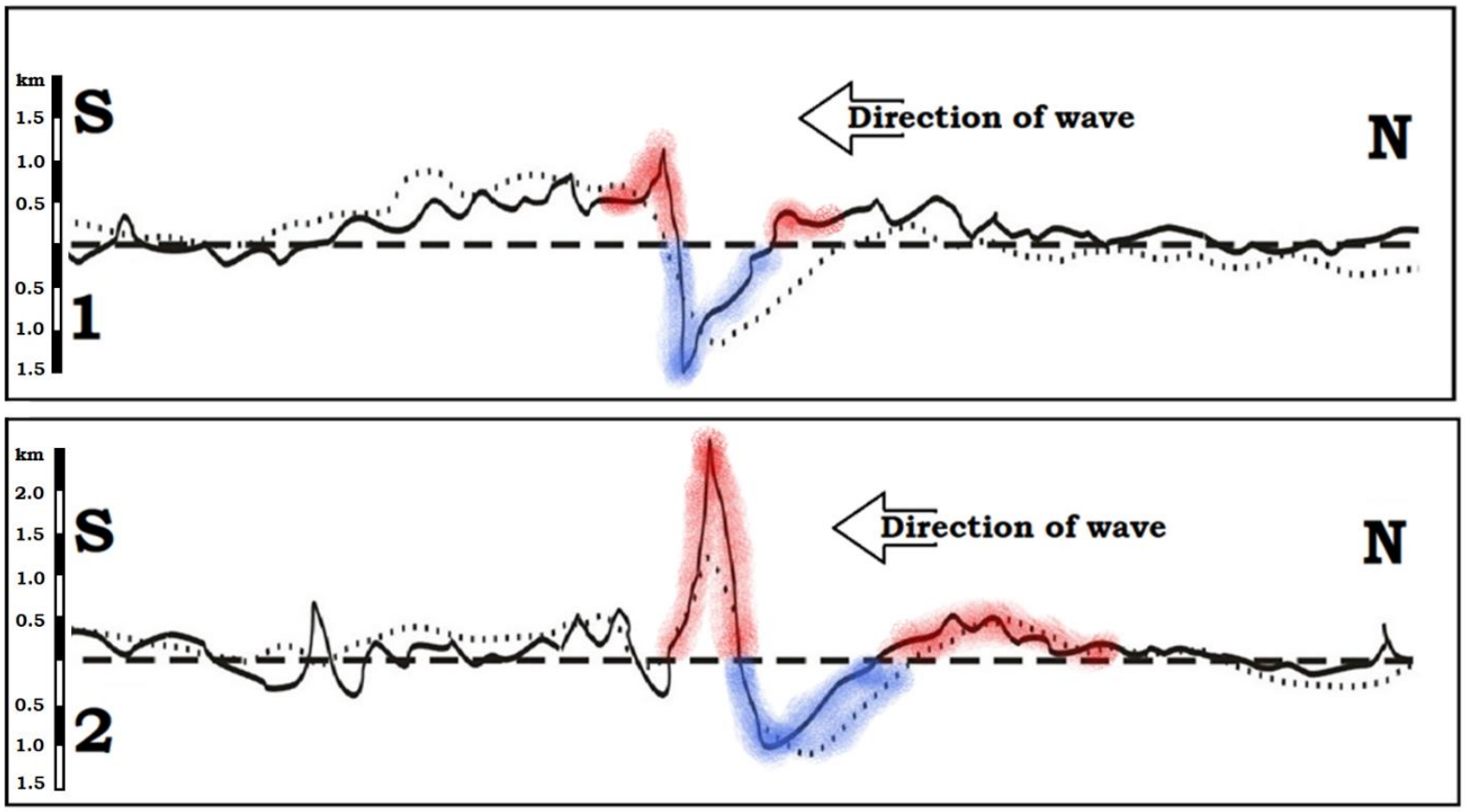

Figure 3.4: S-N cross-sections of Clarion FZ extending ~200 km in each direction from the center of the ridge slope. Dashed line is an arbitrary median for deviation. Solid line is bathymetry (topography) and dotted line is free-air gravity anomaly readings. Locations 1 and 2 from Figure 3.3. (Image credit: Modified from Bonneville and McNutt 1992).

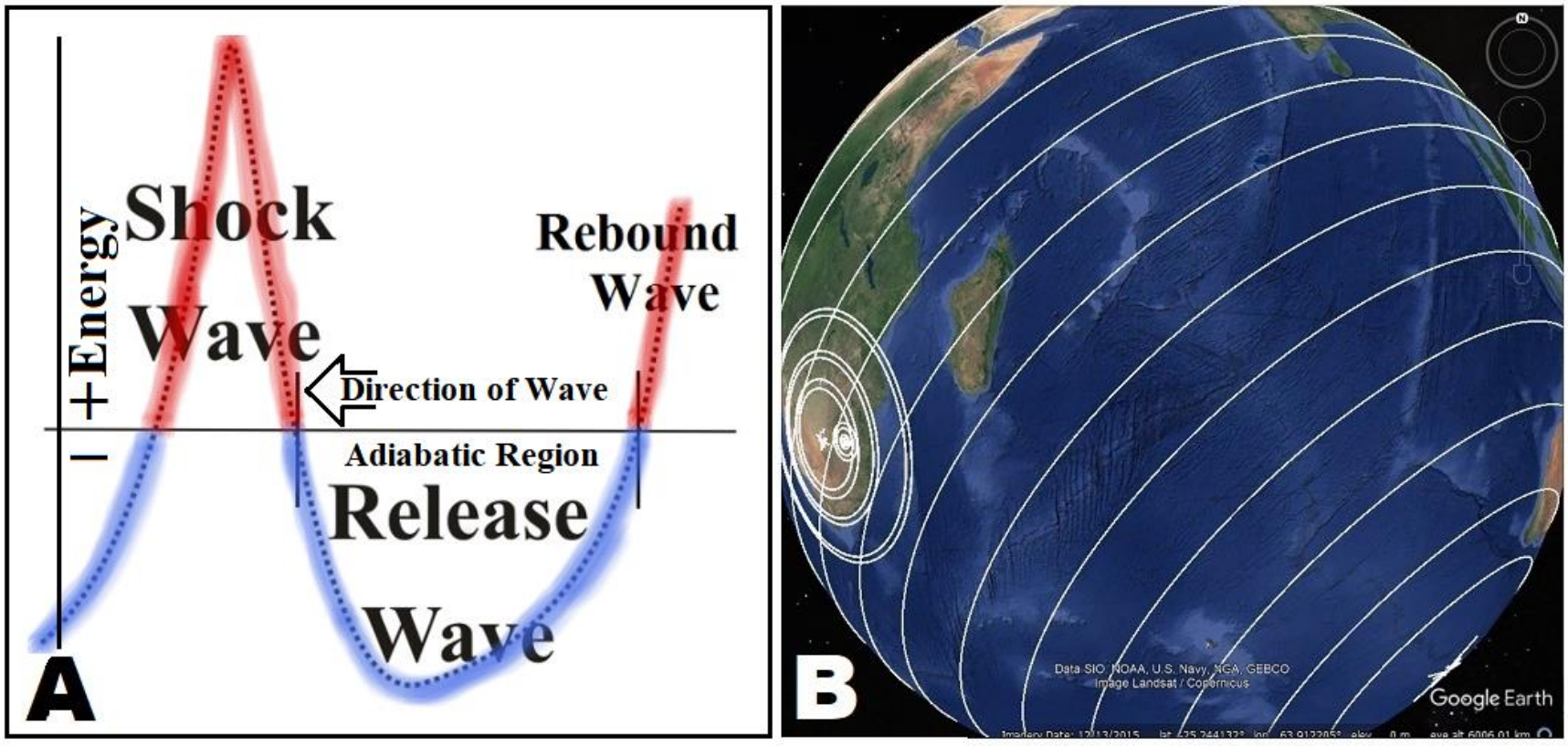

Figure 3.5: (A) Standard shock-release wave profile (B) Globe of earth showing how circular lineaments around a point turn to small circle rings with greater distance and are often perceived as straight lineaments at earth's surface (Teubner, et al 2017, Barnhart 2017).

Krakatoa's wave pair

The 1883 eruption of Krakatoa volcano in Indonesia was reported to be the largest shock wave in recorded history. While it excavated a pit less than 8 km (5 miles) diameter, forty-five seismic stations worldwide recorded the shock wave's passing and 8 preserved a tracing of the shape of the wave (Figure 3.6). The shock wave consisted of 3-4 smaller burst of energy and an equal number of dips in the following rarefaction/release wave. The pairing of high and low portions identifies it as a shock-release wave. Additionally, the general shape matches the energy wave shape shown in Figure 3.5, with the sudden rise and immediately following greater drop in energy levels showing the adiabatic response.

The quality of the wave record diminished with distance and repetitions (time). It circled the globe at 36 hours and 24 minute intervals for 5.6 days until it could not be distinguished from background noise. As a wave continues, its shape varied more from noise than energy dissipation.

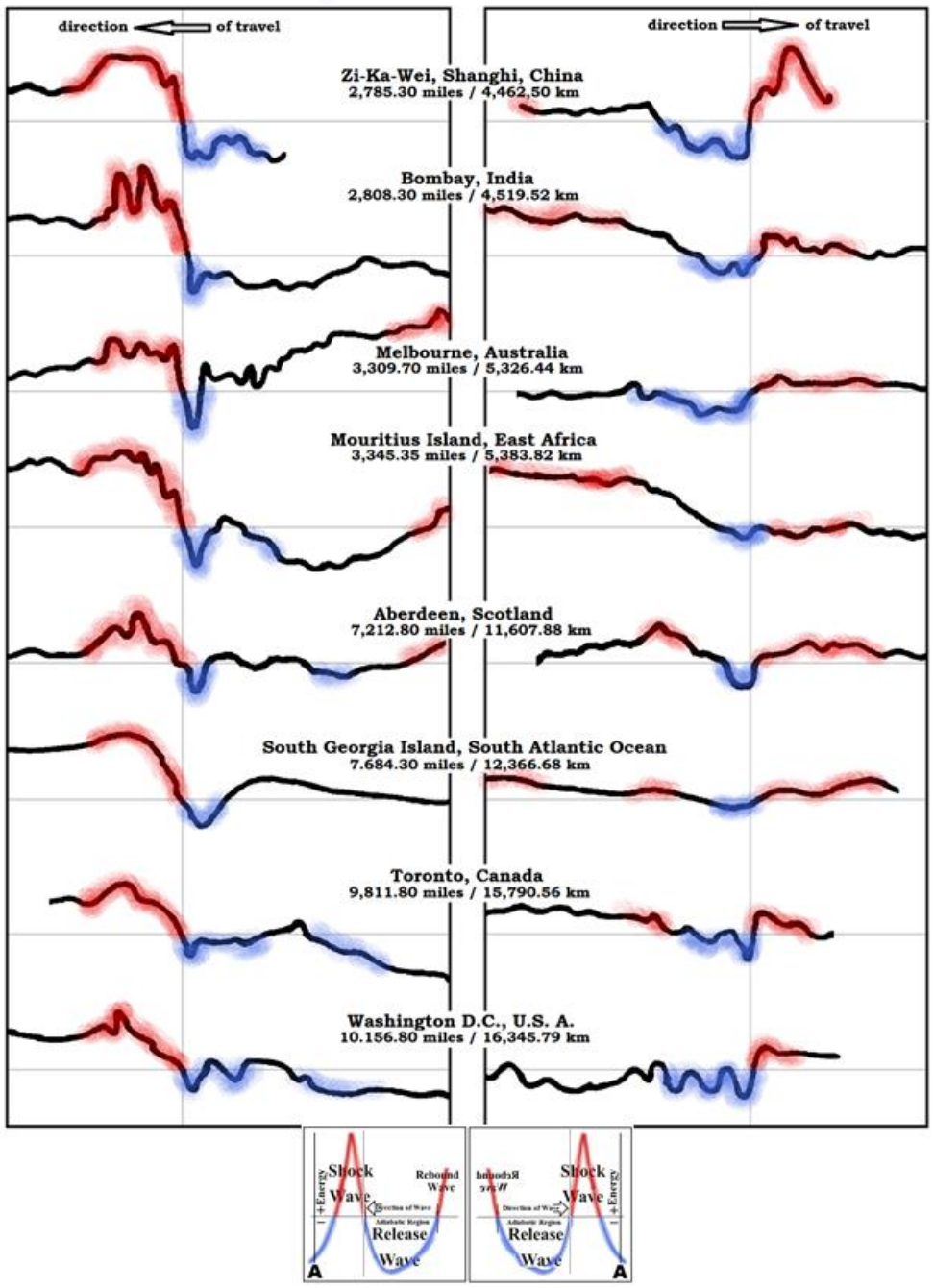

Figure 3.6: Record of wave shapes recorded around the globe after the Krakatoa eruption of 1883. (Image redrawn from Symons 1888)

Figure 3.7 shows a power boat on a fjord. While five wave patterns, probably reflections from distant shores, can be recognized outside of the wake, the same patterns can be seen within the wake (detail B) after the “noise”--energy of the boat’s motor-- has been superimposed on them. The energy pattern of the wave is not destroyed, only subjected to constructive and destructive interference being added.

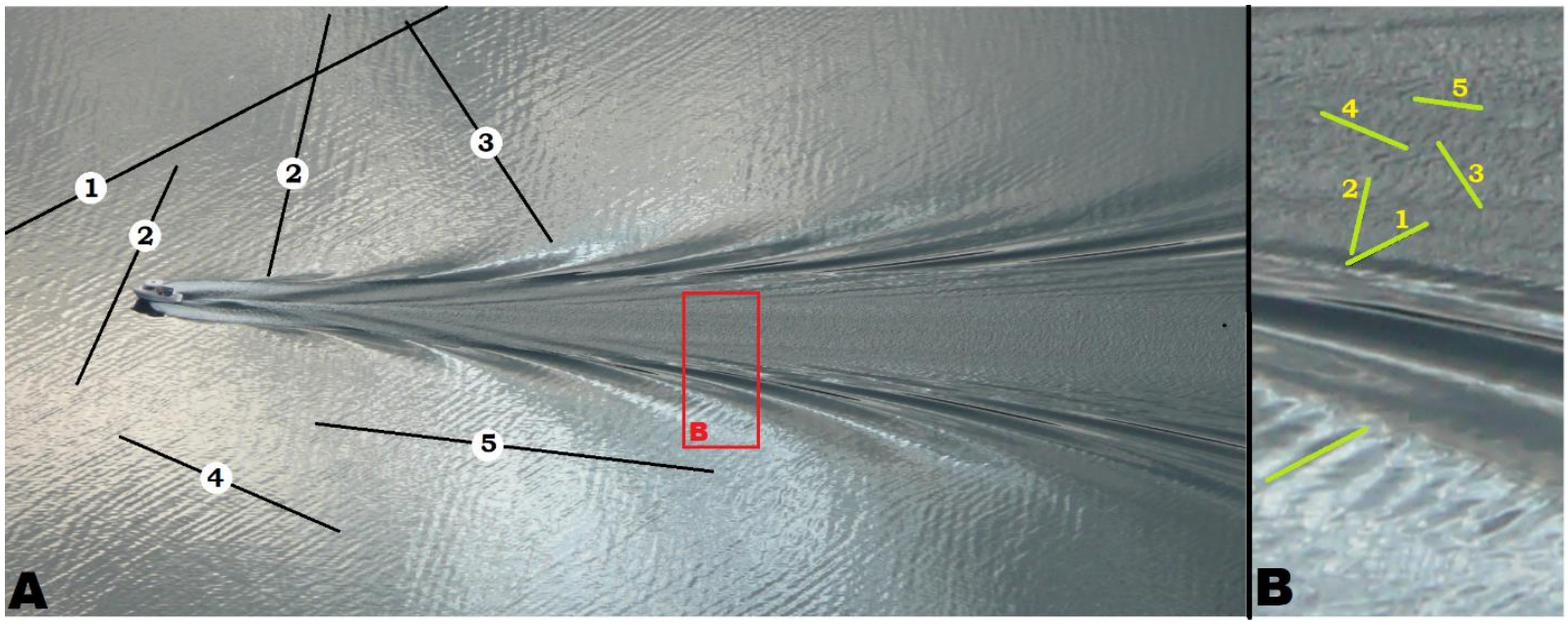

Figure 3.7: Boat motoring on Lyna Fjord, Norway, photographed from Preikestolen, showing constructive and destructive interference patterns are conserved across and inside of the wake in detail B. (Image credit: Edmont 2009.)

Locating the Pacific FZ center

As any three points define a small circle line on a sphere, using a program by Maarten ‘t Hart (personal communication) which locates lines on Google Earth, three points were designated on the high side of the FZ’s trenches (Figure 3.8) with the coordinates of each point shown in Table 1.

Rather than locating a center of rotation, I would designate the center of a ring, the point where an astral-impactor struck and its antipode. If this ring is a complete ring, this center was the source of the shear that formed the ring just like the Krakatoa volcano was the source of the shock waves recorded around the world. The difference seen between Krakatoa and the Pacific FZ is that the FZ had much more energy behind the wave so that it thrust-up a mountain ridge and was not just a passing shock wave. If that stress was identified as a volcanic explosion like Krakatoa, earthquake, or some kind of cryptoexplosion (French 1998), most readers would have no problem accepting it. Why should we have trouble accepting an astral–impactor which delivers considerably more energy to a shear point?

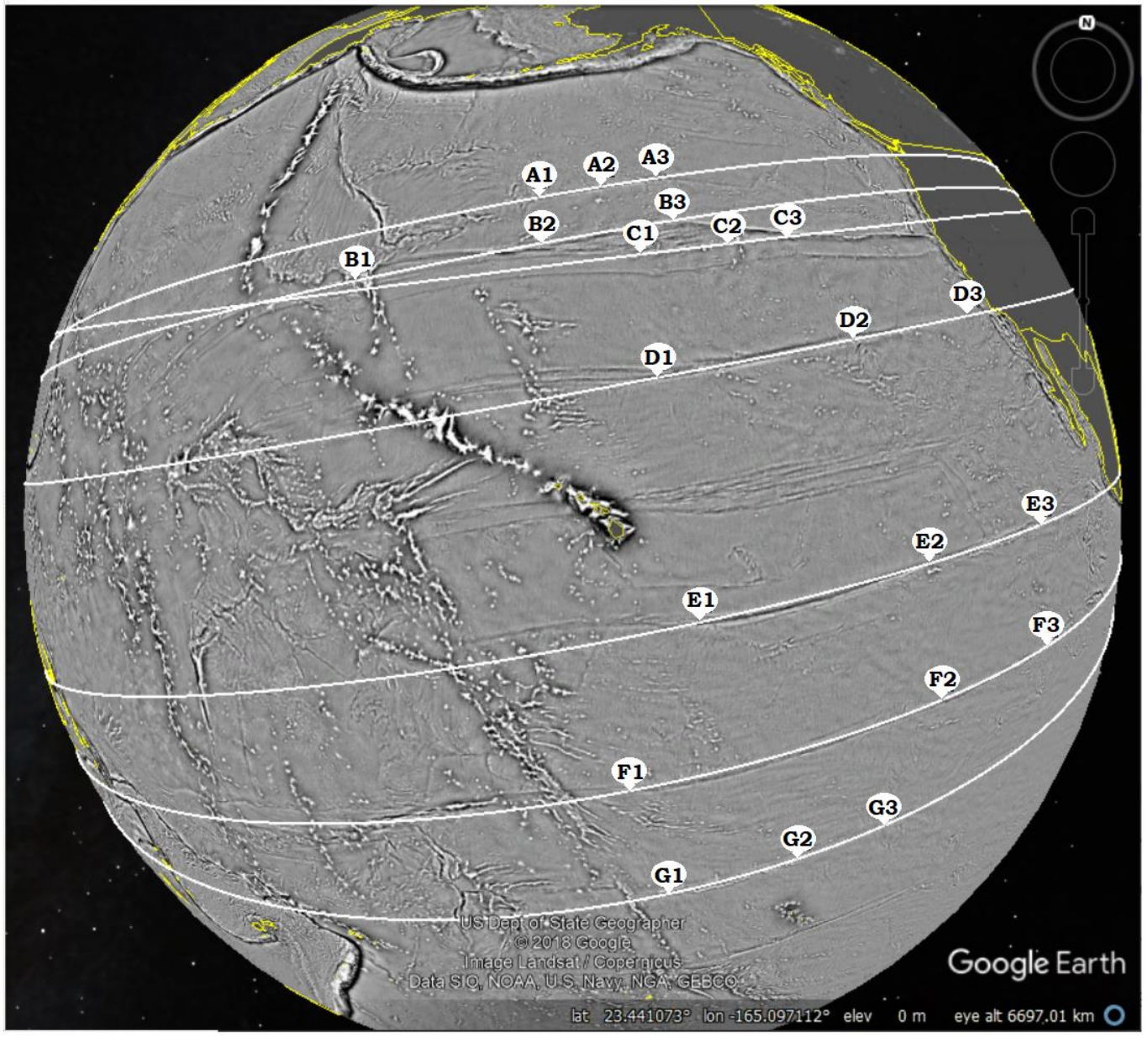

Figure 3.8: The Pacific FZ in Vertical Gravity Gradient showing the locations of the points chosen on each FZ and the lines they produced. (Image credit: Google Earth overlay. Scripps 2014.)

Realizing very small changes in location of any of the three points, would vary the center located for the line, and the lines produced from the shortest segments would likely produce the most deviation, centers C and G were excluded. Centers A-E are grouped in Figure 3.9A.

	1 Latitude	1 Longitude	2 Latitude	2 Longitude	3 Latitude	3 Longitude	Center Latitude	Longitude
A	41.250974°	-163.623286°	42.556769°	-158.175926°	43.618966°	-153.276311°	70.432510°	72.323252°
B	33.733173°	-177.100639°	37.775471°	-162.719050°	40.269483°	-151.967071°	71.006161°	74.762602°
C	37.564250°	-154.572310°	38.804028°	-147.180975°	39.623109°	-141.710611°	76.873620°	81.894498°
D	29.276497°	-153.069049°	32.295535°	-137.319876°	33.964209°	-124.199295°	71.719883°	76.549212°
E	14.107099°	-149.748123°	17.160409°	-132.597500°	18.334717°	-120.003194°	69.103245°	69.549277°
F	2.681643°	-153.348419°	7.409584°	-130.736089°	8.915680°	-118.720982°	71.864519°	78.639925°
G	-5.754978°	-149.848317°	-3.500313°	-140.871882°	-1.897996°	-134.040300°	74.900437°	103.448147°

Table 3.1: Latitude and longitude coordinates of points mapped on Figure 3.5

While C Center is in the midst of a fairly complete circular linear which is near the rotational center located by Morgan, I will associate that ring with the Kara crater, Figures 3.9B and 2.15-17. Viewing the clustering of the remaining 6 centers, I felt it was too close for random occurrences. Believing the impactor for the Pacific FZ was larger than later impactors, like the Kara (920 km/ 570 mi diameter) that overlapped it, I searched for indication of another possible center in that area in Global Gravity Anomaly (Figure 3.10), which included land surfaces.

I chose the center labeled in Figure 3.9B. While Figure 3.9B shows several rings indicated in the bathymetry, the most recognizable pattern is where the Kara and the Pacific rings overlapped within the red circle.

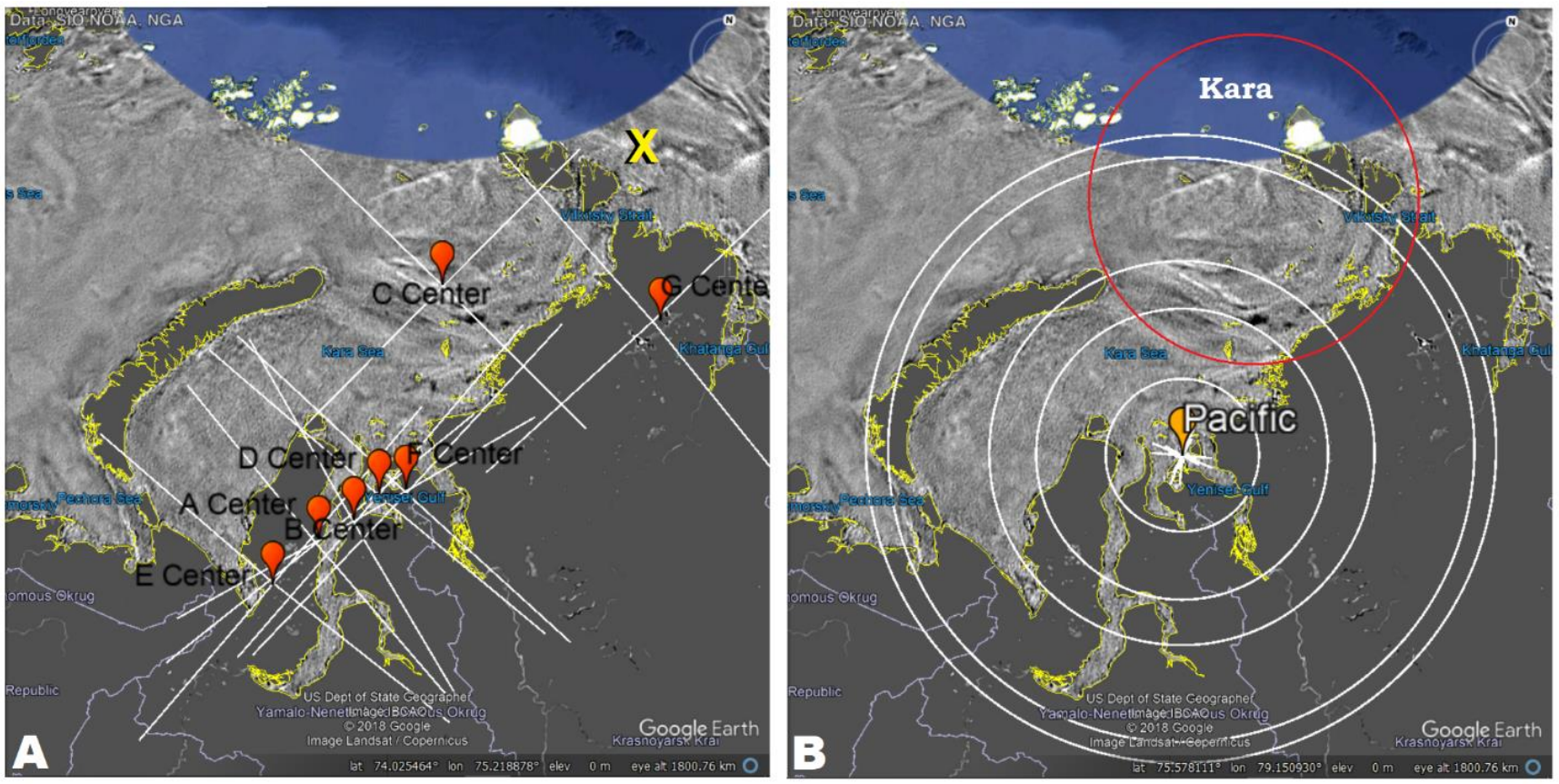

Figure 3.9: Vertical Gravity Gradient overlay for Google Earth image of the Kara Sea north of Siberia. (A) Locations of centers mapped with three points for each line. Yellow X near the northeast corner is the rotational center at 79ºN and 111ºE located by Morgan (1968). (B) Some of the rings indicated by bathymetry and gravity measurements for PFZ center. Note the interaction of both centers in the area of the red ring. (Image credit Google Earth © 2019)

On a global gravity anomaly map (Scripps 2014), Figure 3.10, linears are indicated by the changes in gravity reading. Looking back at Figure 3.5 for the shape of a shock-release wave, the most drastic change takes place in the precipitous drop from the shock wave's escarpment high to the extreme low of the release wave. With adequate detail, this drastic change point in the gravity reading should show higher reading on the outside of the FZ linear and lower reading on the inside of that linear. This is clearly visible in the Kara rings, Figure 3.9B, and the Clarion bathymetry, Figure 3.3B and C.

	Latitude N	Longitude E	Distance from last ring		Fracture Zones
Center	72.7085°	78.0330°			
A	35.1545°	159.0067°	6,000 km	3,700 mi	Chinook
B	38.9217°	-157.4193°	900 km	560 miles	Mendocino
D	29.6688°	-152.5439°	2,100 km	1,300 mi	Murry
	22.7052°	-144.9364°	920 km	572 miles	Molokai
E	15.3950°	-142.0826°	860 km	534 miles	Clarion
F	4.3549°	-144.9628°	1120 km	696 miles	Clipperton
G	-3.7798°	-141.7004°	960 km	597 miles	Galapagos
	-12.5270°	-142.6565°	930 km	578 miles	Marquesas
	-23.7904°	-148.4457°	1050 km	652 miles	Austral

Table 3.2: Using the designated center and a point on each FZ, a map of the Pacific Fracture Zone linears can be reproduced by the reader.

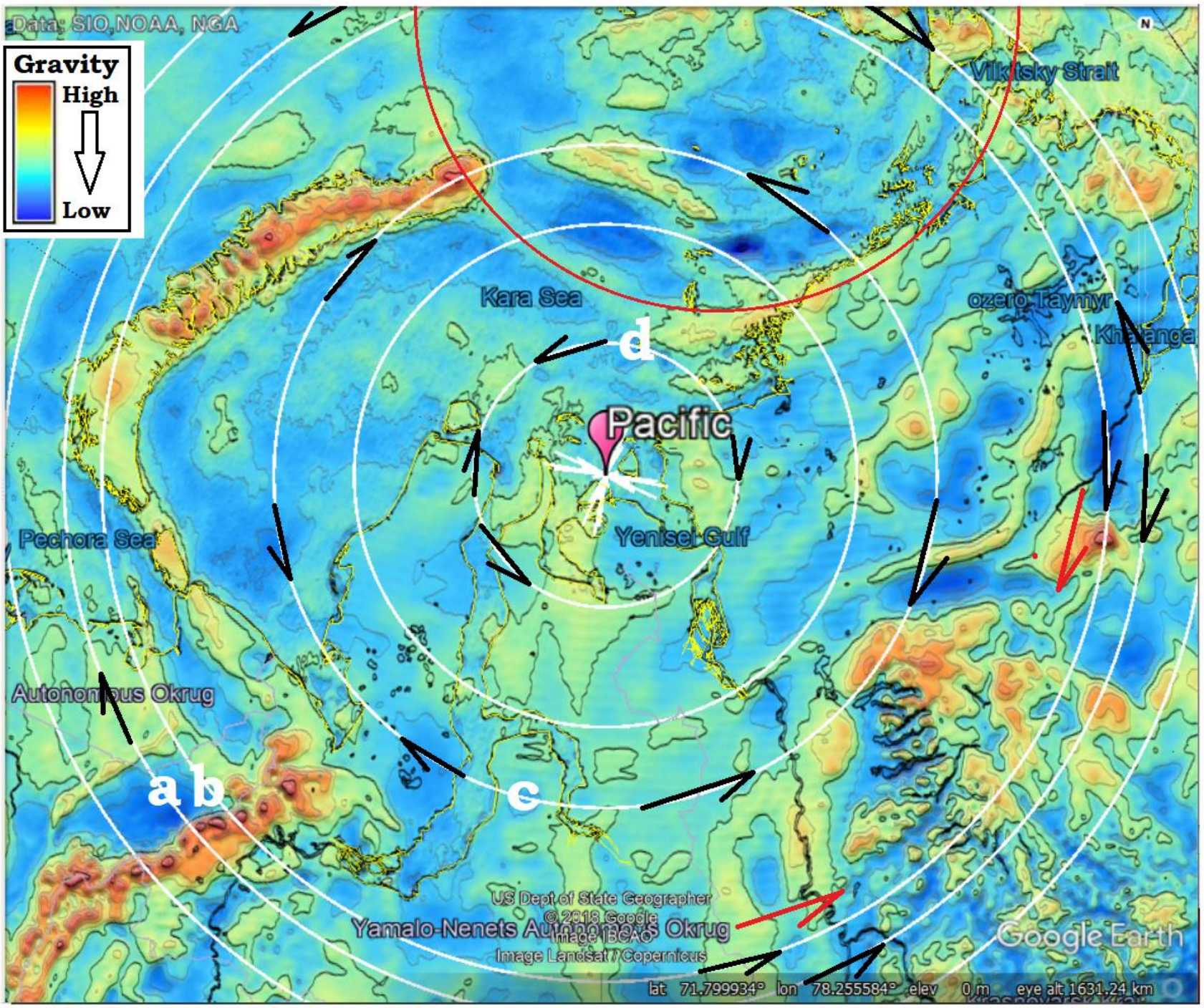

Figure 3.10: Global Gravity Anomaly showing some of the gravity change points which identify the circular lineament around the Kara rings. The “a” ring probably represents the original cratering rim or primary upthrust of the shock wave. (Image credit: Global Gravity Anomaly, Scripps 2014).

The Kara RPC

The Kara original crater rim is 980 km (600 mi) in diameter. Its circular lineament is possibly the most distinct on the ocean floor. This suggest it was one of the later impacts for its size. Where it overlaps the Pacific center the pattern is consistent with cumulative interference patterns, typical of water drops in a lab’s ripple tank, when two sets of ripples cross (Figure 3.11). That this pattern is several hundreds of kilometers wide testifies to the size and energies of impactors involved, and response of earth’s lithosphere to that great energy, much like water in a pond. With multiple impactors like the Kara adding to the pattern, it starts to be obvious why the rings of the Pacific center are much more elusive, and we need to look for more than a simple ring when dealing with evidence of one of the earliest impactors.

The interaction of the Kara ring and Pacific center also speaks to the timing of the impacts. They did not have millions of years in between. In a time line that long, any latent energy would likely be dissipated and energy signatures would not interact. Even if only thousands of years separated the impacts, clear patterns like this would not be expected. These interactions then point to interaction timeframes of a few days to weeks. This suggest that a heavy bombardment of impactors within the yearlong Flood is a viable alternative.

Figure 3.11: Ripples on a pond resulting from a series of water drops.

Compared to multi rings craters on the Moon, Nectarous?

Hartmann and Kuiper (1962) recognized three rings around Mare Nectarous at radii of 200 km, 300 km, and 420 km. They identified the third as heaviest in the southwest quadrant with Rupes Altai or Altai Escarpment, the largest escarpment on the moon. While the Altai Escarpment does not completely encircle Mare Nectarous, it is easily traced between superimposed craters for more than a quarter of the circle and with individual outcropping mountains for the rest of the ring. As folded mountains do not occur on the moon (Hartmann and Kuiper 1962) with an absence of tectonic forces, any mountains outside obvious craters rims will need an explanation. This would make all mountains on the moon as expressions of underlying energy directly traceable back to an impact's shear center. Therefore the occurrence of concentric ring even at very great distance, may be difficult to recognize, but it is very likely.

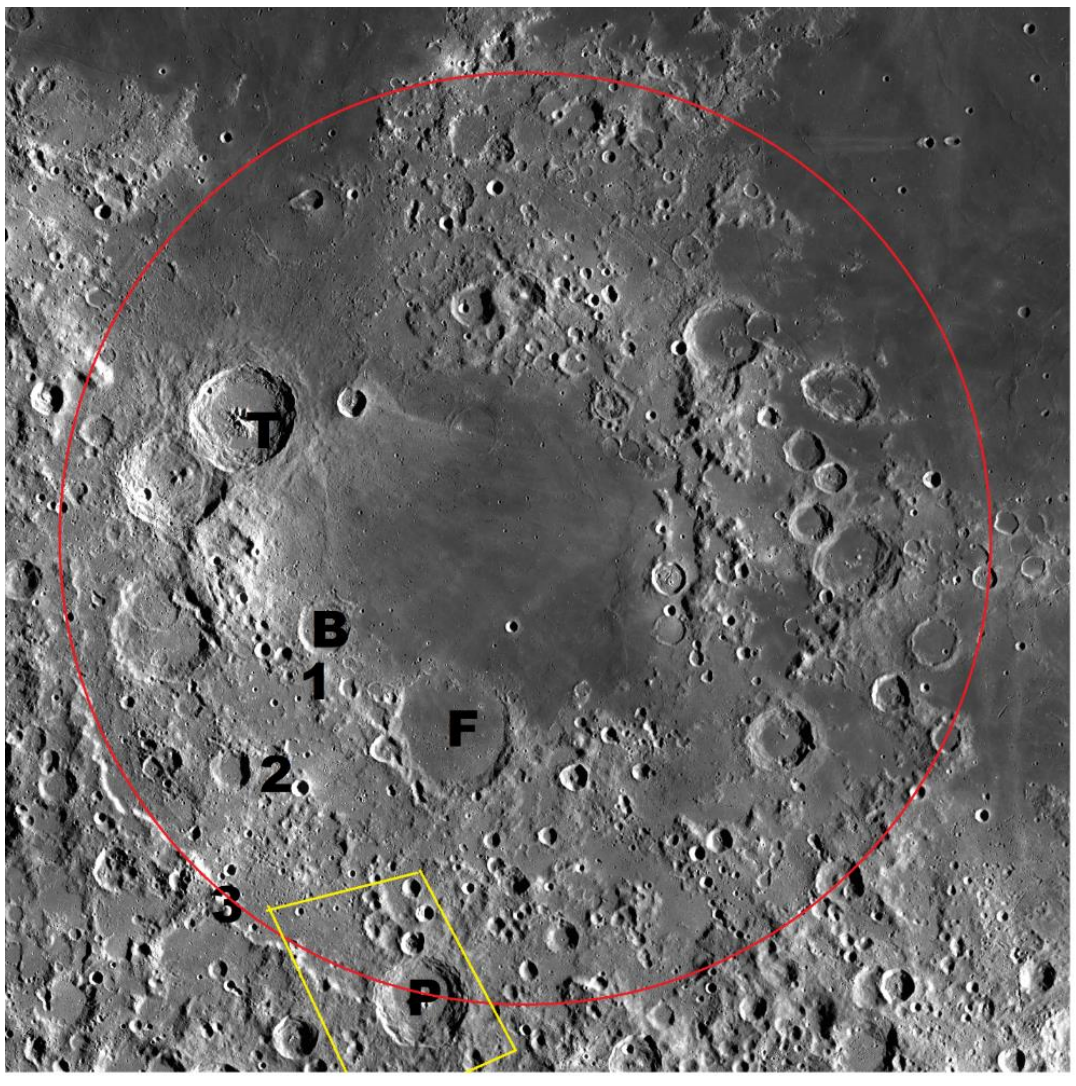

Figure 3.12: Mare Nectarous, its three recognized rings and a few smaller included craters. T= Theophilus, B= Beaumont, F= Fracastorius, P= Piccolomini. Yellow trapezoid, area of Figure 3.14 detail. (Image credit: JMARS NASA 2014)

But, not only can the mountains be traced to impact centers, the distortions of the rings of mountains is accounted for with overlying craters. Looking at the portion of the Altai Escarpment going north from the Piccolomini crater within the yellow quadrilateral in Figure 3.12, the scarp is pushed southwest into an arc with a small crater at its center. The small crater is not responsible for the movement, but the arc lines up to a lowered portion of the northwest rim of the Piccolomini (Figure 3.13, shown in yellow in the second image) and a smaller ring (shown in red) which distorts both larger rings. Each successive crater is not a blasted hole that

destroys any energy signature in its way, but as *a ripple in the surface*, simply *adds its own energy signature to the pattern already present*.

Although the original ring from Mare Nectarous is distorted within the smaller craters, Figure 3.13, an enlarged detail, Figure 3.14, shows a trend of small ridges, possibly lithologic differences, at the ring's original location.

The distortion of the Altai scarp by these two ghost craters suggest that much distortion of the rings are due to later impacts. If each impact puts energy into uplifting a rim with the shock wave, followed by a ring of lowered energy (topographic features) in the release wave, Figure 3.2, the interacting rings would cause cumulative energy patterns consistent with wave ripple patterns, Figure 3.9, in a short period of time.

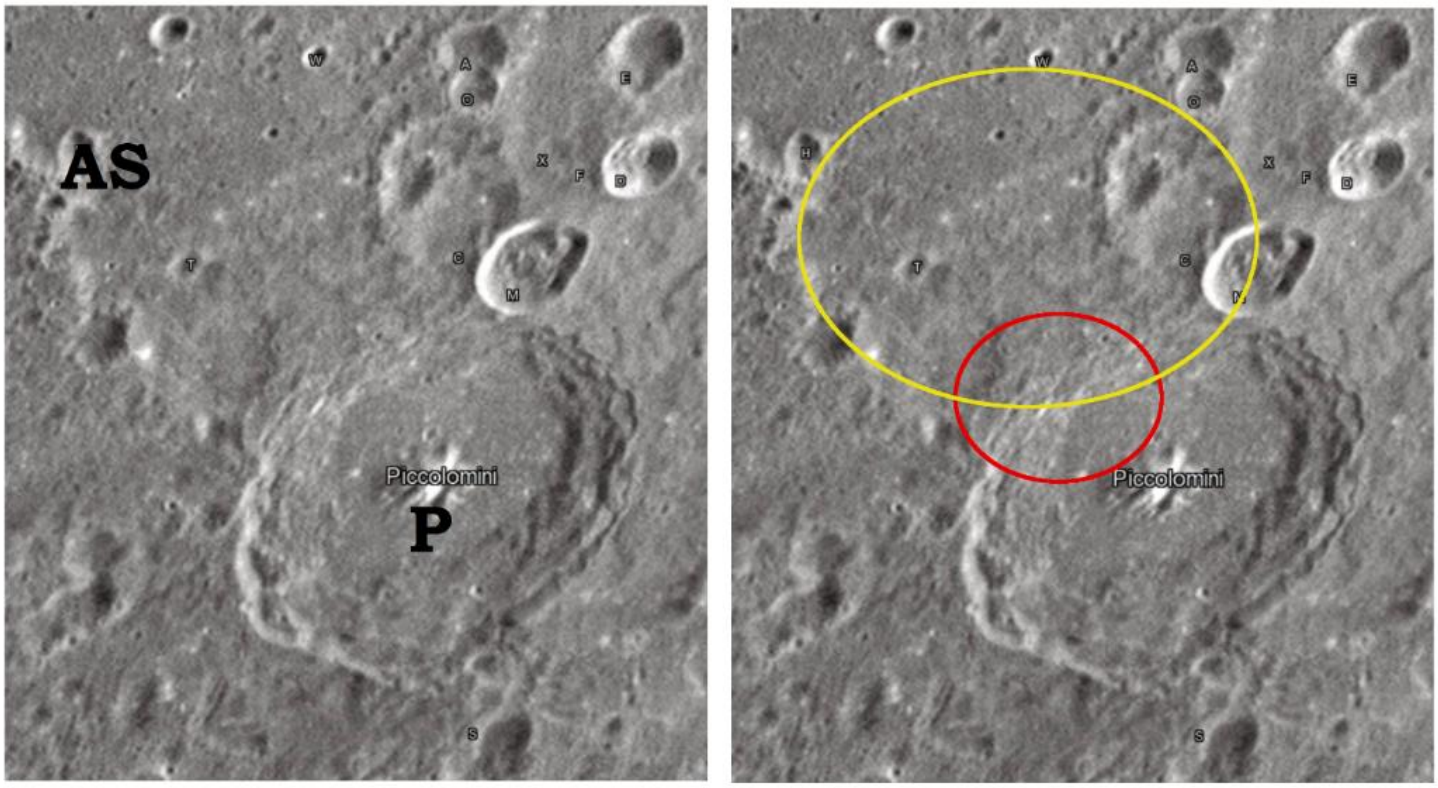

Figure 3.13: Detail of Mare Nectarous around Piccolomini (P) crater showing how ghost craters distort Altai scarp ring. (Image credit: D. Campbell, University of Hertfordshire Bayfordbury Observatory, 2012, CC.)

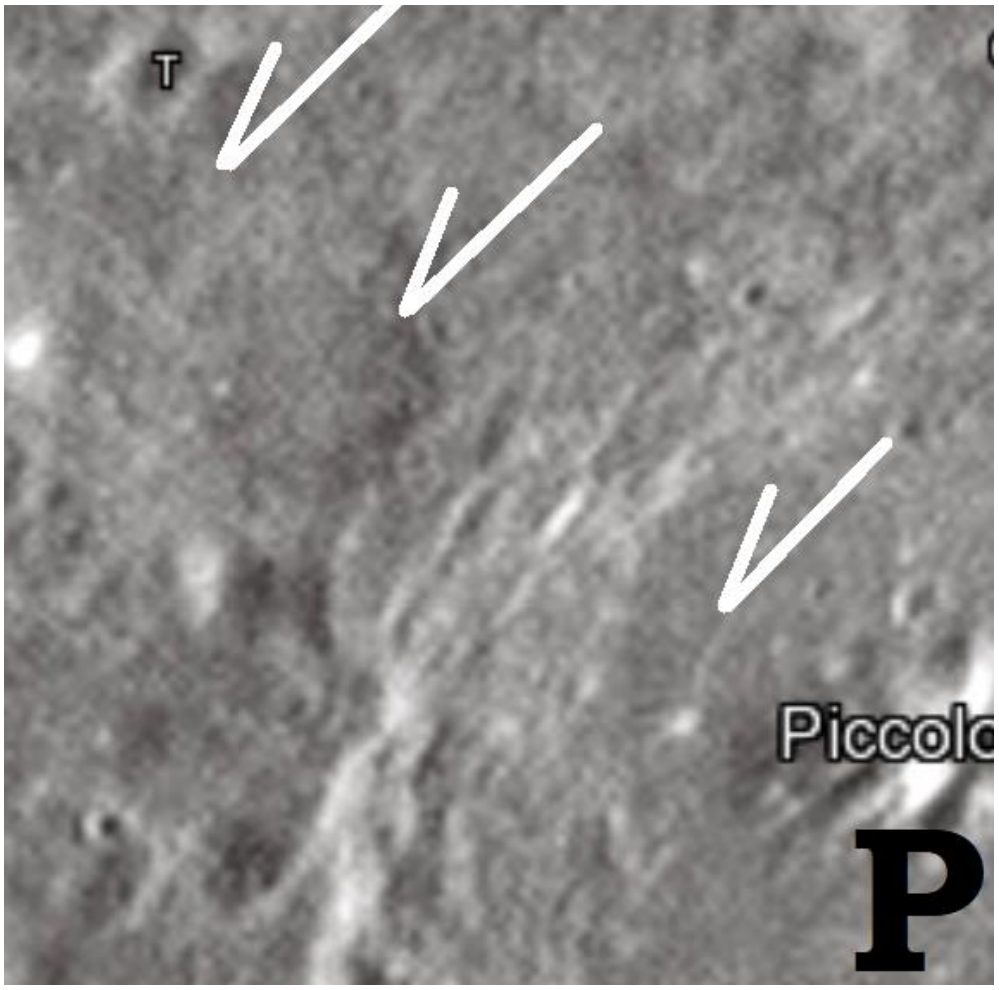

Figure 3.14: Linear of the Altai ring for Mare Nectarous northwest of the Piccolomini crater and separated from the scarp seen in Figure 3.13. Northwest to southeast linears from original ring are pervasive and persistent. (Image credit: Detail from where all three circles in Figure 3.13 overlap. Ghost crater lines omitted for clarity.)

Altai scarp and Clarion FZ

Viewing the Altai scarp obliquely from the north, the direction of the wave (Figure 3.16A), and the sudden rise of 2-3 km. is very conspicuous. Maybe less conspicuous is the ring of flattened ground inside the scarp ring. It has a small ridge on the inside edge, possibly the inside edge of the adiabatic envelope.

The Clarion FZ structure is directly compares to the Altai scarp except for the massive number of smaller craters that are not obscuring the Pacific ring in this area. For some reason this area of the Pacific basin was spared many of the later impacts or our imaging lacks sufficient resolution.

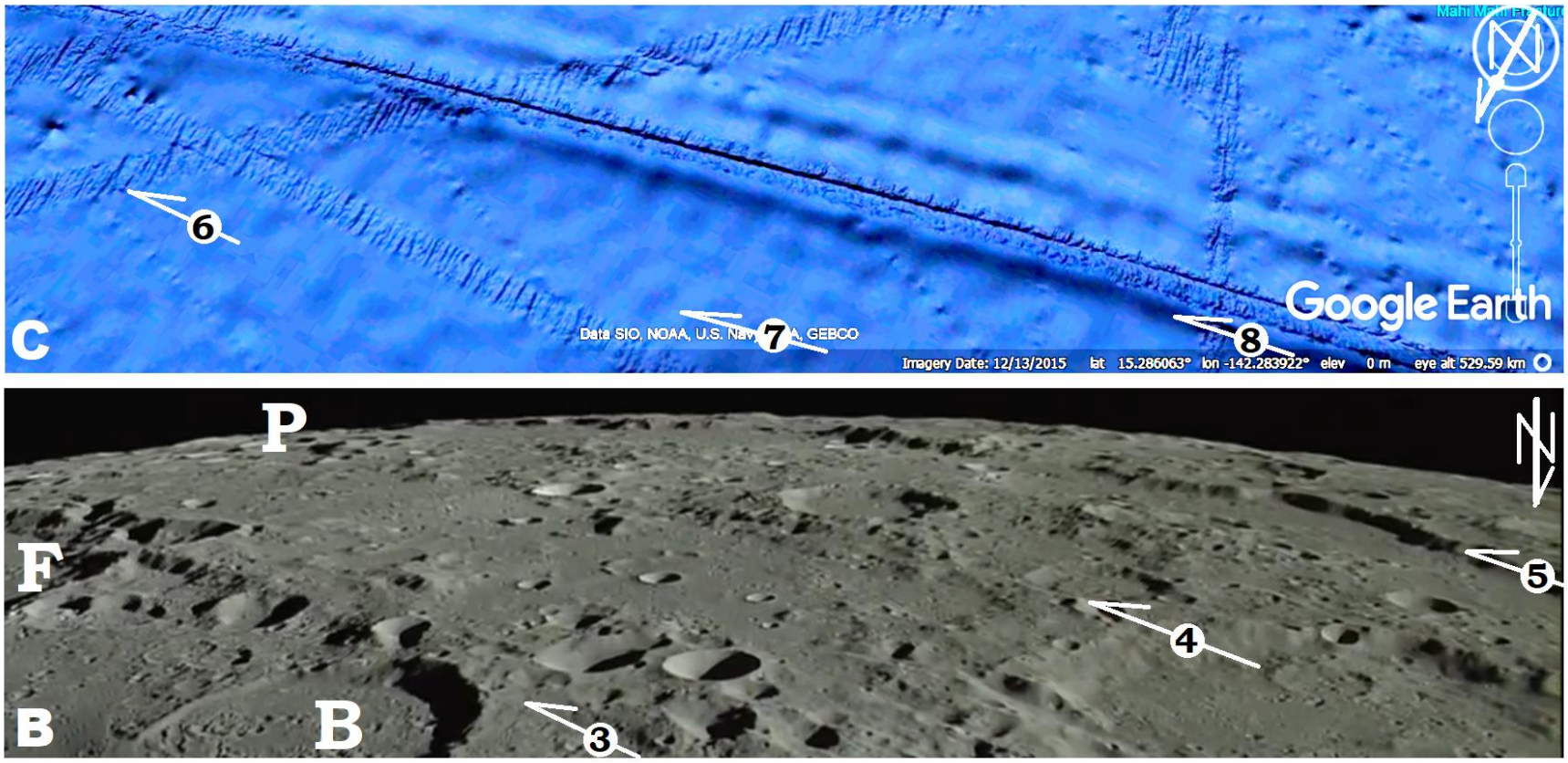

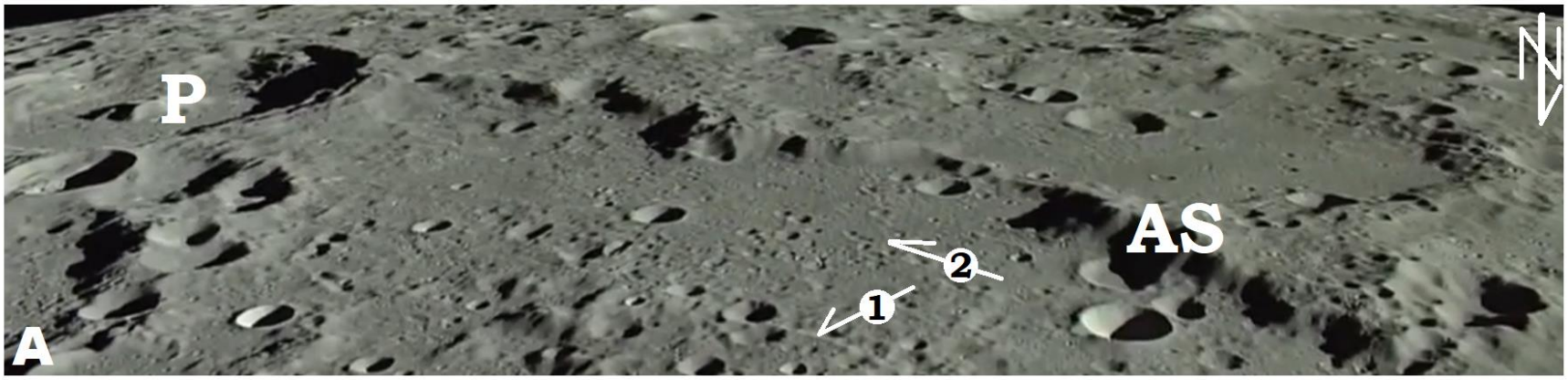

Figure 3.15: Oblique view of Altai scarp (AS). (A) 1- Inside edge of adiabatic envelope, 2- Linears within release wave that are concentric to Nectarous center. (B) 3-Inside ring Nectarous, 4- Second ring of Nectarous, 5- Third ring of Nectarous (Craters same abbreviation as Figure 13). (C) 6- Trackways of extra data at higher resolution, 7- linears concentric to ridge inside release valley, 8- Scarp of Clarion FZ. (Images credit: (A&B) JAXA/NHK, 2020. © Google Earth 2018)

Mare Orientale

Hartmann and Kuiper (1962) identifies 5 rings for Mare Orientale with their radii: Inner Montes Rook ring- 160 km. (100 mi), Montes Rook ring- 240 km. (150 mi), Cordillera ring- 310 km. (193 mi), Eichstadt ring- 465 km, (290 mi), Rocca ring- 750 km. (466 mi). I have added 6 more rings going out to about 1400 km. (870 mi) radius, and indicated in Figure 3.12 ridges and strings of mountains seen as concentric to Orientale. Without plate tectonics on the Moon, there is no tectonic folding, so crater rims and concentric ring structures are the only source of mountains. If the reader does not want to recognize these ridges and mountains as concentric to Orientale, then what other source is available for their orogeny?

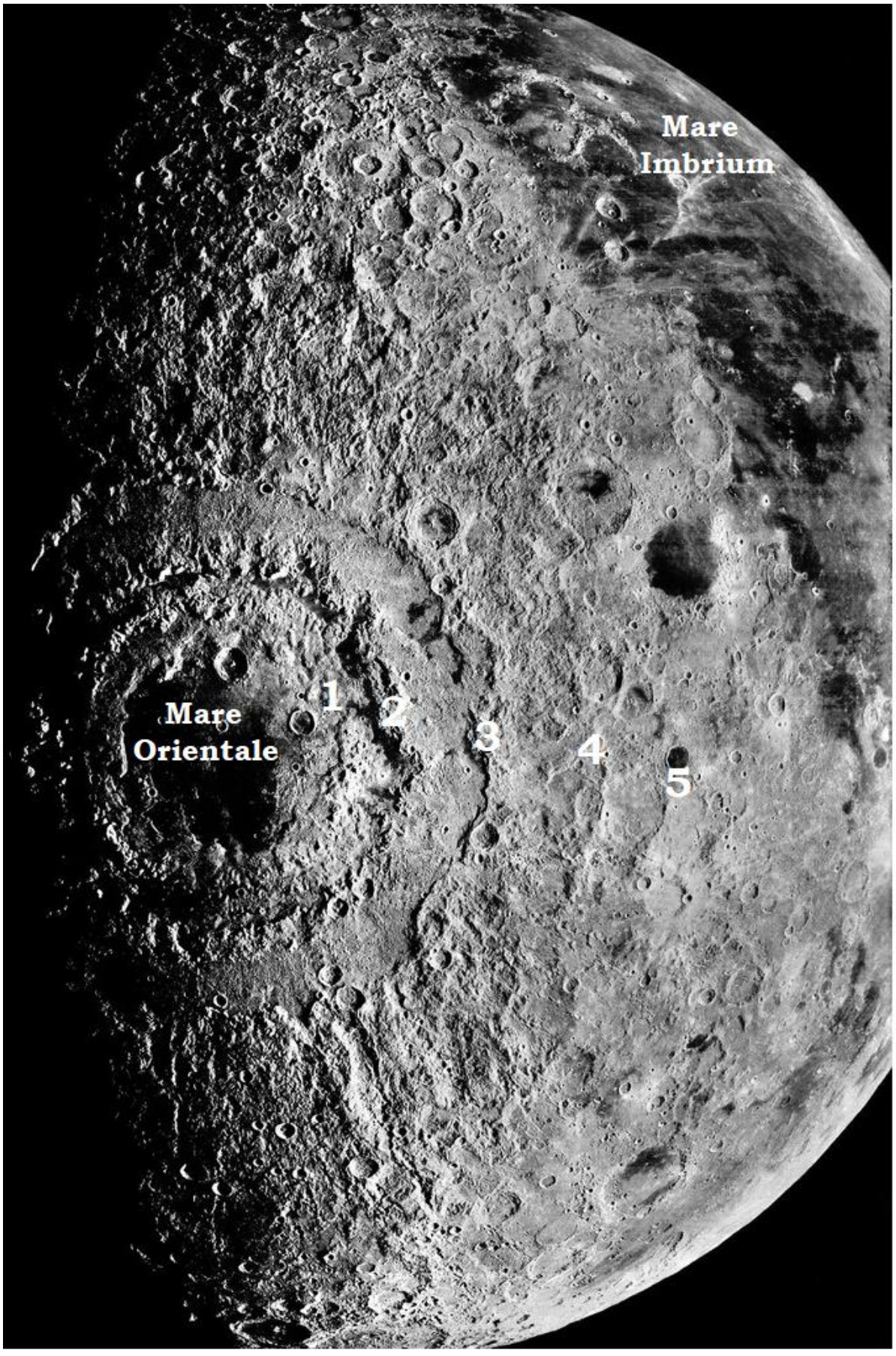

Figure 3.16: Mare Orientale lying to the south west of the Mare Imbrium basin. The five rings recognized by Hartmann are labeled. (Image credit: NASA)

Using Red Relief map, a coloring used to emphasize elevation changes (JAXA/NHK 2020) seven more rings are located at approximately the same wave length. Many areas of these rings are marked between white arrows on Google Moon (Figure 3.17A) and made visible in Red Relief by similar red lines as the first 5 rings.

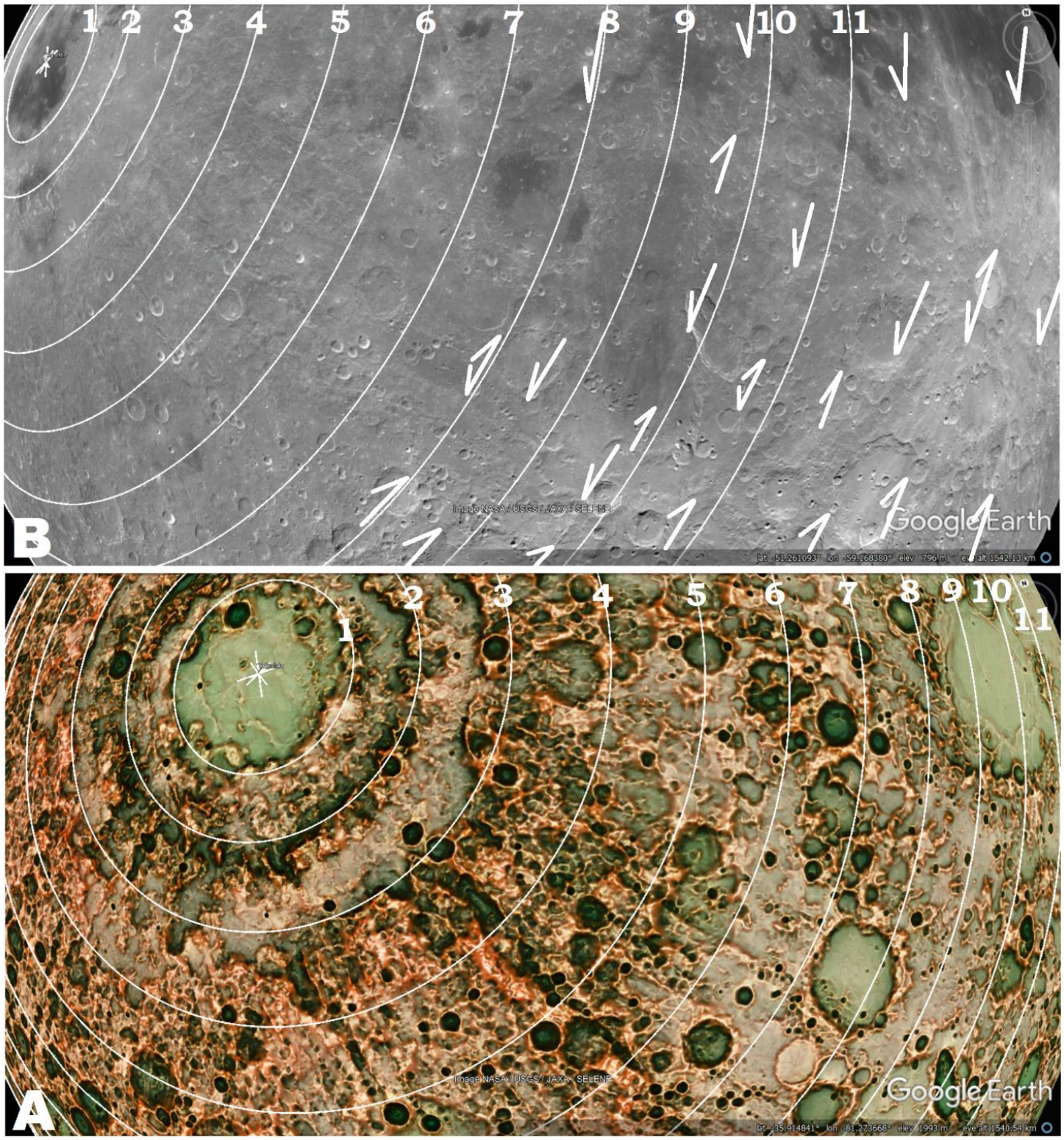

Figure 3.17: (A) Red Relief overlay to Google Earth of the Orientale basin complex with exaggerated relief intervals. (B) Google Earth Moon image of the same area with some of the more major concentric relief features marked between white arrows. (Image credit: (A) Chiba et al 2008, (B) Moon, ©Google Earth 2020.)

Conclusion

In the early 1960's astronomers were hesitant to recognize impact cratering on the moon, because that would suggest the lunar geomorphology came about in a different manner than that on the earth. Are we in the opposite situation now?

Is an astral-impact the only explanation for the 9 concentric linears of the Pacific FZ? I am sure it is not, but I cannot think of any other viable explanation. The likelihood of 9 concentric lines would form over 9,000 km (5,600 miles) at roughly the same interval, wave length, without a wave source of shear seems improbable. A source of sheer that is large enough to produce the energy to raise mountains over 1 kilometer (0.6 miles) tall over 13,700 km (8,500 miles) distant in the Austral FZ seems improbable. Making the assumption that the same forces shaped the Earth as the Moon. Impact produced scarps on the Moon bear a striking similarity to the Pacific FZ's structure. How likely are they to be produced by a different source of shear?

We need to ask ourselves, if the Pacific FZ structure were found on the Moon or Mars, would anyone have trouble suggesting it was astral-impact related? Of course we have to recognize that were the craters on the moon found on the earth, they may well not be recognized as astral-impact craters, because we have no idea what form the shock induced changes would take in multi-ringed craters of that size. Once again, a fresh look at the details of the Pacific FZ show the Creator is in those details, and the plate tectonics model for Earth's geomorphology needs to be reconsidered.

References

Atwater, T. 1970. Implications of Plate Tectonics for the Cenozoic tectonic evolution of Western North America, The *Geological Society of America Bulletin* 81:3513-3536.

Atwater, T., J. Sclater, D. Sandwell, J. Severinghaus, M.S. Marlow. 1993. Fracture Zone traces across the North Pacific Cretaceous Quiet Zone and their tectonic implications. In *The Mesozoic Pacific: Geology, Tectonics, and Volcanism.* Pringle, M. S., W. W. Sager, W. V. Sliter, and S. Stein. (editors), American Geophysical Union, Washington, D. C. pp 137-154.

Austermann, J, Z. Ben-Avraham, P. Bird, O. Heidbach, G. Schubert, and J.M. Stock. 2011. Quantifying the forces needed for the rapid change of Pacific plate motion at 6 Ma. *Earth and Planetary Science Letters* 307:289-287.

Austin, S., J. Baumgardner, R. Humphreys, A.A. Snelling, L. Vardiman, and K.P. Wise, 2010. Catastrophic Plate Tectonics: A global Flood model of Earth History. https://answersingenesis.org/geology/plate-tectonics/catastrophic-plate-tectonics-global-flood-model-of-earth-history/, accessed 7/2/2019.

Barnhart, W.R. 2017. Cratering and the Earth: Finding a cause in Earth's lineaments, *Creation Research Society Quarterly* 53(1):191-205.

Bonneville, A. and M. McNutt. 1992. Shear strength of the great Pacific fracture zones. *Geophysical Research Letters*. 19(20): 2023-2026.

Chiba, T., S. Kaneta, Y. Suzuki. 2008. Red Relief Image Map: New visualization method for three dimensional data, *The International Archive of the Photogrammetry, Remote Sensing and Spatial information Science*, 37(Part B2):1071-1076. Asia Air Survey Co., Kawasaki, Japan.

French, B.M. 1998. *Traces of Catastrophy: A Handbook of Shock-Metamorphic Effects in Terrestrial Meteorite Impact Structures.* LPI Contribution 954. Lunar and Planetary Institute, Houston. 120p.

Hartmann, W.K. and G.P. Kuiper. 1962. No.12 Concentric structures surrounding Lunar Basins. *Communications of the Lunar and Planetary Lab* 1:51-66.

Hoffman, P.F. 2014. Tuza Wilson and the acceptance of pre-Mesozoic continental drift, *Canadian Journal of Earth Science* 51:197-207.

JAXA/NHK. 2020. "KAGUYA taking "Rupes Altai" by HDTV" https://www.youtube.com/watch?v=dJA-U6ICXeY, accessed 1/2/2020.

Jones, A.P., G.D. Price, N.J. Price, P.S. DeCarli, and R.A. Clegg. 2002. Impact induced melting and the development of large igneous provinces. *Earth and Planetary Science Letters* 202 (3–4):551–561.

McCarthy, M.C., S.E. Kruse, and M.R. Brudzinski. 1996, Changes in plate motions and the shape of Pacific fracture zones, *Journal of Geophysical Research*, 101(B6):13,715-13,730.

Morgan, W.J. 1968. Rise, Trenches, Great faults and Crustal Blocks. *Journal of Geophysical Research* 73(6):1959-1982.

Pezeril, T., G. Saini, D. Veysset, S. Kooi, P. Fidkowski, R. Radovitzky and K. A. Nelson. 2011. Direct Visualization of Laser-Driven Focusing Shock Waves, *Physical Review Letters* **106** (21) – Published 24 May.

Scripps Institute of Oceanography. 2014. Global [Marine] Gravity Anomaly download. http://topex.ucsd.edu/grav_outreach/. Accessed 11/19/2014,

Symons G. 1888. *The eruption of Krakatau and subsequent phenomena: Reports of the Krakatau Committee of the Royal Society*. Trubner, London.

Teubner, U., Y. Kai, T. Schlegel, D. E. Zeitoun, and W. Garen. 2017. Laser-plasma induced shock waves in micro shock tubes, *New Journal of Physics*. 19.

Wilson, J. Tuzo. 1965. A new class of faults and their bearing on Continental Drift. *Nature*, 207(4995):343-347.